Modeling Nonwetting-Phase Relative Permeability Accounting for a Discontinuous Nonwetting Phase

Ulrich Fischer,* Olivier Dury, Hannes Flühler, and Martinus Th. van Genuchten

ABSTRACT

A model for the wetting- and nonwetting-phase constitutive relationships is presented. The nonwetting-phase relative permeability in the model is a function of the degree of continuous nonwetting-phase saturation. Different formulations of the continuous nonwetting-phase model were evaluated by comparison of calculated and measured air permeabilities as well as discontinuous air saturations. A Brooks and Corey–Burdine type formulation of the nonwetting-phase relative permeability was more accurate than the corresponding van Genuchten–Mualem equation. Estimated discontinuous air saturations were higher for drying than for wetting, thus reflecting hysteresis in the water-retention and relative air permeability functions. The continuous nonwetting-phase model provided a much better prediction of relative air permeabilities than a formulation that neglects the presence of a discontinuous nonwetting phase. The emergence point model for the nonwetting-phase relative permeability provided a good approximation of the continuous nonwetting-phase model.

TWO-PHASE AS WELL AS MULTIPHASE FLOW has long been of interest in petroleum production. Because of an increase in the number of spills of nonaqueous-phase liquids (NAPLs) into the subsurface during the last decades, multiphase flow has also become an important topic in soil physics and hydrology. Besides the infiltration of NAPLs into soil, such remedial procedures as soil vapor extraction, air sparging, and soil flushing also deal with multiphase flow.

Two-phase flow models not only differ in the calculation of permeability but also vary in the definitions of residual and effective saturations. The relative permeability of a porous medium to a given phase in a multiphase system is generally considered to be a function of the degree of saturation of that phase. Since at high wetting-phase saturations, the nonwetting phase may be discontinuous with a considerable fraction of nonwetting phase being trapped (e.g., Stonestrom and Rubin, 1989a), the nonwetting-phase permeability should be a function of the continuously distributed nonwetting-phase saturation, rather than the total nonwetting-phase saturation. Lenhard and Parker (1987) described the nonwetting-phase relative permeability as a function of the continuous nonwetting-phase saturation and of the corresponding apparent wetting-phase saturation, the latter being the sum of the wetting-phase saturation and those amounts of nonwetting phase that do not contribute to nonwetting-phase flow.

U. Fischer, Dep. of Civil Engineering and Operations Research, Princeton Univ., Princeton, NJ 08544; O. Dury, and H. Flühler, Inst. of Terrestrial Ecology, Swiss Federal Inst. of Technology ETH, Grabenstr. 3/11a, CH 8952 Schlieren, Switzerland; and M.Th. van Genuchten, U.S. Salinity Lab., USDA-ARS, 450 W. Big Springs Road, Riverside, CA 92507-4617. This work was conducted at the Inst. of Terrestrial Ecology, Swiss Federal Inst. of Technology, Schlieren, Switzerland. Received 31 Oct. 1996. *Corresponding author (fischer@karst.princeton.edu).

Published in Soil Sci. Soc. Am. J. 61:1348–1354 (1997).

In practice it is difficult to separate the total nonwetting-phase content into continuous nonwetting phase (which should be connected to at least two open boundaries of the domain under consideration), a locally accessible nonwetting phase (connected to only one open boundary), and a trapped nonwetting phase (connected to none of the open boundaries). Stonestrom and Rubin (1989a,b) determined the locally accessible air content and the relative air permeabilities of two soil materials as a function of water saturation. For zero air permeability, the difference between total air and locally accessible air accounted completely for trapped air. For air permeabilities greater than zero, the nontrapped fraction of air could not be separated into continuous and locally accessible air. We will use the term *discontinuous nonwetting phase* to refer to the sum of trapped and locally accessible nonwetting phases.

Stonestrom and Rubin (1989b) investigated the dependence of air permeability on water saturation and introduced the term *emergence point* for the water saturation where air flow first becomes detectable during drying, and the term *extinction point* for the water saturation where air flow first becomes unmeasurable (zero) during wetting. Several previous experimental studies on multiphase flow have shown that flow of the nonwetting phase could be detected only as long as the wetting-phase saturations did not exceed about 70 to 80% (e.g., Odeh, 1959; Corey, 1957; Morgan and Gordon, 1970; Stonestrom and Rubin, 1989b). Despite these data sets showing the important effect of a discontinuous nonwetting phase, to our knowledge only Fischer et al. (1996) presented a comparison of nonwetting-phase permeability data and calculations obtained with parametric models that accounted for the presence of a discontinuous nonwetting phase. These same researchers presented an empirical model of the nonwetting-phase relative permeability that is based on the knowledge of the emergence or extinction point.

The objective of this study was to develop a model of the wetting- and nonwetting-phase constitutive relationships accounting for a discontinuous nonwetting phase, and to evaluate the capability of this model to describe nonwetting-phase relative permeabilities and discontinuous nonwetting-phase saturations. Different formulations of the continuous nonwetting-phase model were evaluated by comparison of calculated and measured air permeabilities as well as discontinuous air saturations. We also compared the proposed model to other models describing nonwetting-phase relative permeability, and studied how well these models approximate the continuous nonwetting-phase concept.

Abbreviations: BCB, Brooks and Corey–Burdine; CNP, Continuous Nonwetting Phase; EP, Emergence Point; TNP, Total Nonwetting Phase; VGM, van Genuchten–Mualem.

THEORY

Parametric Model for Two-Phase Flow Accounting for a Discontinuous Nonwetting Phase

In our parametric model for two-phase flow, we considered only single branches of the wetting and drying retention and permeability functions. The relationship between the positive value of the matric potential head, h, and the effective wetting-phase saturation, $\bar{S}_w$, is described by the model of van Genuchten (1980):

$$\bar{S}_w = [1 + (\alpha h)^n]^{-m} \quad [1]$$

where α, n, and m are empirical parameters, and $\bar{S}_w$ is defined as

$$\bar{S}_w = \frac{S_w - S_{w,r}}{S_{w,s} - S_{w,r}} \quad [2]$$

in which S_w is the wetting-phase saturation, $S_{w,r}$ is the residual wetting-phase saturation, and $S_{w,s}$ is the maximum wetting-phase saturation. The relationship between matric potential head and effective apparent wetting-phase saturation, $\bar{S}_{w,a}$, is modeled either with a van Genuchten type equation:

$$\bar{S}_{w,a} = [1 + (\alpha_a h)^{n_a}]^{-m_a} \quad [3]$$

or according to the model of Brooks and Corey (1964):

$$\bar{S}_{w,a} = \left(\frac{h_a}{h}\right)^{\lambda_a} \quad \text{for } h > h_a \quad [4a]$$

$$\bar{S}_{w,a} = 1 \quad \text{for } h < h_a \quad [4b]$$

where α_a, n_a, m_a, h_a, and λ_a are empirical parameters, and $\bar{S}_{w,a}$ is defined as

$$\bar{S}_{w,a} = 1 - \bar{S}_{n,c} = \frac{S_{w,a} - S_{w,r}}{1 - S_{w,r}} \quad [5]$$

in which $\bar{S}_{n,c}$ is the effective continuous nonwetting-phase saturation, and $S_{w,a}$ is the apparent wetting-phase saturation. As shown in Fig. 1 for an air–water system, the difference between $S_{w,a}$ and S_w is the discontinuous nonwetting-phase saturation, $S_{n,d}$:

$$S_{n,d} = S_{w,a} - S_w \quad [6]$$

Wetting-phase relative permeability, $k_{w,r}(\bar{S}_w)$, is modeled as a function of $\bar{S}_w$ since it was concluded that hysteresis in wetting-phase permeability is insignificant (e.g., Demond and Roberts, 1987, 1993) and is described as a combination of the van Genuchten retentivity model and the conductivity model of Mualem (1976) to give, for fixed $m = 1 - 1/n$ (van Genuchten, 1980),

$$k_{w,r}(\bar{S}_w) = (\bar{S}_w)^a [1 - (1 - \bar{S}_w^{1/m})^m]^2 \quad [7]$$

in which exponent a is a fitting parameter accounting for the effects of tortuosity and connectivity with respect to the wetting phase. Mualem (1976) found that a value of 0.5 provided a good average of the relative water permeability for many soils.

Lenhard and Parker (1987) presented a model for the relative air permeability that was derived by application of the van Genuchten–Mualem (VGM) approach (Mualem, 1976; van Genuchten, 1980) to the air phase and accounts for discontinuous air. Their equation can be written as a general model for the nonwetting phase relative permeability, $k_{n,r}(\bar{S}_{n,c})$, giving for fixed $m_a = 1 - 1/n_a$:

$$k_{n,r}(\bar{S}_{n,c}) = (\bar{S}_{n,c})^b [1 - (1 - \bar{S}_{n,c})^{1/m_a}]^{2m_a} \quad [8]$$

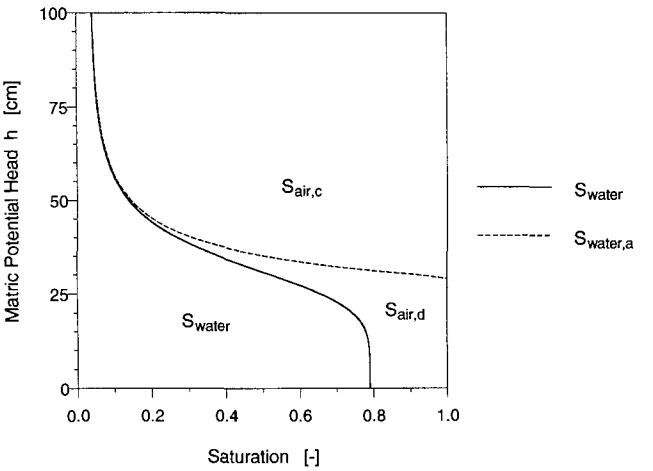

Fig. 1. Domains of water saturation, S_{water}, discontinuous air saturation, $S_{air,d}$, and continuous air saturation, $S_{air,c}$. The two air domains are separated by the function of apparent water saturation, $S_{water,a}$. The curves were obtained for the data measured for the quartz sand mixture and pure water during drying and using the Brooks and Corey–Burdine formulation of the Continuous Nonwetting Phase (CNP_BCB) model for calculating $S_{water,a}$ (cf. Fig. 2).

where exponent b accounts for tortuosity and connectivity with respect to the nonwetting phase. The corresponding equation obtained by applying the Brooks and Corey–Burdine (BCB) approach (Burdine, 1953; Brooks and Corey, 1964) is

$$k_{n,r}(\bar{S}_{n,c}) = (\bar{S}_{n,c})^b [1 - (1 - \bar{S}_{n,c})^{1+2/\lambda_a}] \quad [9]$$

The Continuous Nonwetting Phase (CNP) models of the nonwetting-phase relative permeability represented by combination of either Eq. [3], [5], and [8], or Eq. [4], [5], and [9], are referred to as the CNP_VGM model and the CNP_BCB model, respectively. In predictions, we used a value of 0.5 for b in the CNP_VGM model and a value of 2.0 in the CNP_BCB model.

Alternative Models for the Nonwetting-Phase Relative Permeability

As already pointed out, the amount of continuous nonwetting phase (or apparent wetting phase) is difficult to measure. Therefore, the nonwetting-phase relative permeability is frequently described as a function of the total nonwetting-phase saturation. The assumption that any nonzero nonwetting-phase saturation, $S_n = 1 - S_w$, allows advective flow of the nonwetting phase leads to the following concept presented originally by Parker et al. (1987) for the modeling of relative air permeability:

$$k_{n,r}(\bar{S}_n) = (\bar{S}_n)^b [1 - (1 - \bar{S}_n)^{1/m}]^{2m} \quad [10]$$

in which the effective nonwetting-phase saturation, $\bar{S}_n$, is given as

$$\bar{S}_n = \frac{S_n}{1 - S_{w,r}} \quad [11]$$

This model is referred to as the Total Nonwetting-Phase (TNP) model.

Recently, Fischer et al. (1996) presented an equation for calculating relative air permeability that can be written in a generalized form as a model of the nonwetting-phase relative permeability based on knowledge of the emergence or extinction point of the nonwetting-phase flow, $S_{w,e}$ (and therefore further referred to as the Emergence Point [EP] model):

Table 1. Summary of gas permeability data. The values of $h(S_{w,e})$ were calculated from the fitted water retention curves for which the van Genuchten parameters α and m were obtained. The values of $h_s(S_{w,e})$ were calculated according to Eq. [14].

No.	Reference†	Soil material	Wetting fluid	Process	$S_{w,s}$	$S_{w,r}$	$S_{w,e}$	$h(S_{w,e})$	$h_s(S_{w,e})$	α	m
								cm		cm^{-1}	
1	A	quartz sand mixture	water	drying	0.79	0.04	0.53	30	–	0.031	0.81
2	A	quartz sand mixture	2% butanol	drying	0.78	0.04	0.57	17	19	0.054	0.72
3	A	quartz sand mixture	6% butanol	drying	0.77	0.04	0.59	13	13	0.051	0.81
4	A	quartz sand mixture	water	wetting	0.78	0.04	0.69	13	–	0.081	0.78
5	A	quartz sand mixture	2% butanol	wetting	0.81	0.04	0.73	9	8	0.068	0.79
6	A	quartz sand mixture	6% butanol	wetting	0.80	0.04	0.77	7	6	0.096	0.77
7	B	Oakley sand	water	drying	0.88	0.29	0.77	37	–	0.023	0.82
8	B	Oakley sand	water	wetting	0.87	0.29	0.80	7	–	0.068	0.60

† A: Dury (1997, unpublished data); B: Stonestrom and Rubin (1989b).

$$k_{n,r}(\bar{S}^*_{n,c}) = (\bar{S}^*_{n,c})^b [1 - (1 - \bar{S}^*_{n,c})^{1/m}]^{2m} \quad \text{for } S_{w,r} < S_w < S_{w,e} \quad [12a]$$

$$k_{n,r}(\bar{S}^*_{n,c}) = 0 \quad \text{for } S_w > S_{w,e} \quad [12b]$$

where $\bar{S}^*_{n,c}$ is an estimate of the effective continuous nonwetting-phase saturation, $\bar{S}_{n,c}$, and is defined as

$$\bar{S}^*_{n,c} = \frac{S_{w,e} - S_w}{S_{w,e} - S_{w,r}} \quad [13]$$

For predictions, we again used a value of 0.5 for b in the TNP and the EP models.

EXPERIMENTAL DATA

The different constitutive relationships were tested using water-retention and air permeability data obtained for two quartz sands. Stonestrom and Rubin (1989a,b) (numerical values and additional experimental details are given in Stonestrom [1987]) investigated Oakley sand, and Dury (1997, unpublished data) used an artificial quartz sand mixture and implemented the experimental procedure presented by Fischer et al. (1996). The constitutive relationships in both studies were determined for wetting as well as drying. In addition to pure water, the constitutive relationships of the quartz sand mixture were determined using aqueous solutions containing 2 or 6% butanol by weight as the wetting fluid. Relative air permeabilities, $k_{air,r}$, were obtained by normalizing absolute air permeabilities with the permeability value determined at residual water saturation. The relative air permeability data modeled in this study are summarized in Table 1. More details about the experimental procedures are given in the references cited above.

The emergence and extinction points for air flow were determined as the mean values of the lowest water saturation at which air flow could not be detected and the highest water saturation at which air flow was detectable. Parameter optimization was done using least square procedures. The relative permeability models were not fitted to $\log(k_{air,r})$ since this procedure generally resulted in a poor description of high permeability data and in most cases the improvement in the description of low permeability data (compared with fitting $k_{air,r}$) was limited to one single permeability value. Fitted parameter values are given in Tables 1 and 2.

RESULTS AND DISCUSSION

Since no data of continuous nonwetting-phase saturations and corresponding nonwetting-phase permeabilities were available, both CNP models could only be fitted to the permeability data selected for this study and no predictions could be done. In this study, two criteria were used to judge the quality of the fits, namely the description of the relative permeability data and how well the calculated emergence or extinction of continuous air, $S_{air,c}$, coincided with the experimentally observed emergence or extinction of air flow. Three parameters (α_a, m_a, and b, or h_a, λ_a, and b) could be optimized in both models. It was found that fitting all three parameters resulted in an only slightly better description of relative air permeabilities than fitting only two parameters. On the other hand, the second criterion was fulfilled much better when $1/\alpha_a$ or h_a were fixed in Eq. [3] and [4], respectively, as the value of the matric potential head at the experimentally determined emergence or extinction point. Therefore this latter option was used in all calculations presented here.

First, we compared both formulations of the CNP model to each other and used this model to estimate discontinuous air and apparent water saturations. Afterward, we compared the CNP model to the TNP and EP models and investigated how well the CNP model could be approximated by TNP and EP models.

Evaluation of CNP Models — Estimation of the Discontinuous Air Saturation

Figure 2 compares relative air permeabilities measured for the quartz sand mixture and for pure water during main drainage with model calculations obtained with both CNP models. The CNP_BCB model describes

Table 2. Parameter values obtained by fitting the Total Nonwetting Phase (TNP), the Emergence Point (EP), and the Continuous Nonwetting Phase (CNP) models to the data listed in Table 1.

Model	Option	Parameter	Data no. 1	2	3	4	5	6	7	8
TNP	b fitted	b	1.8	1.8	1.3	0.85	0.41	0.38	−0.09	0.12
EP	b fitted	b	0.14	0.42	0.26	0.02	−0.18	−0.06	0.15	0.20
CNP_VGM	$\alpha_a = 1/h(S_{w,e})$	m_a	6.3	8.7	5.8	4.6	5.0	5.1	5.6	3.4
		b	3.7	11	5.1	6.9	4.3	4.7	6.0	19
CNP_BCB	$h_a = h(S_{w,e})$	λ_a	4.1	7.4	4.4	3.5	3.6	3.5	4.3	2.4
		b	2.1	9.8	4.2	6.2	3.4	3.4	5.6	19

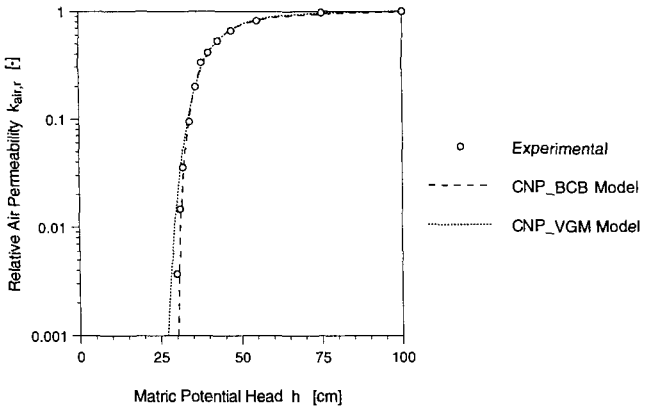

Fig. 2. Comparison of relative air permeabilities determined for the quartz sand mixture and pure water during drying with model calculations using the Brooks and Corey–Burdine (BCB) and van Genuchten–Mualem (VGM) formulations of the Continuous Nonwetting Phase (CNP) model. The parameters h_a and $1/\alpha_a$ were defined as $h(S_{w,e})$ (Table 1) and λ_a, m_a, and b were fitted (Table 2).

the experimental data slightly better than the CNP_VGM model. The corresponding saturations of discontinuous air were calculated with Eq. [6] and are shown in Fig. 3 as a function of water saturation. The total air saturation, S_{air}, and the experimentally determined emergence point are also shown. For water saturations above the emergence point, the discontinuous air saturation should be equal to the total air saturation since no air flow could be detected, and thus no continuous air existed. According to the estimate obtained with the CNP_VGM model, large amounts of continuous air existed already at water saturations above the emergence point. In contrast, the emergence of continuous air as predicted with the CNP_BCB model agrees with the emergence of air permeability. Similar findings as those shown in Fig. 2 and 3 were also obtained for all other investigated data sets. Hence, we conclude that the CNP_BCB model gives the more accurate description of discontinuous air saturation. The curve of apparent water saturation according to the CNP_BCB model is shown in Fig. 1 and compared with the fitted water-retention curve. This plot shows that small amounts of discontinuous air, as indicated by the difference between

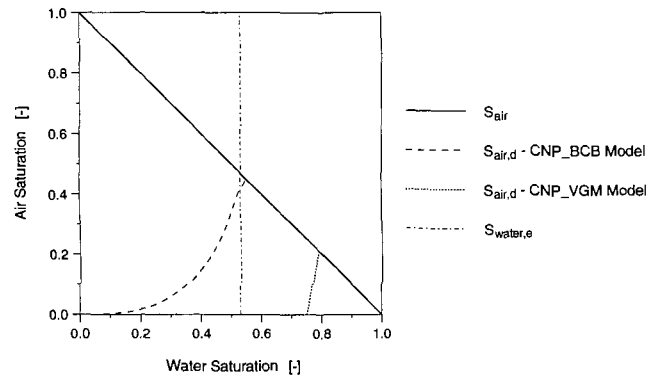

Fig. 3. Discontinuous air saturations, $S_{air,d}$, calculated with Eq. [6] from the model curves shown in Fig. 2. The total air saturation, S_{air}, and the experimentally determined emergence point, $S_{water,e}$, are also shown.

both curves, also existed at relatively low water saturations.

The abruptness of air permeability emergence as reported by Stonestrom and Rubin (1989b) suggests a sudden increase in continuous air saturation at water saturations just below the emergence point. Probably, during drying just prior to the emergence of nonwetting-phase permeability, large amounts of discontinuous nonwetting phase exist and continuity of this phase is impeded by small amounts of wetting phase. Removal of these wetting-phase blockages will then result in an abrupt emergence of the continuous nonwetting phase. Similarly, during wetting at the extinction point, small amounts of wetting phase separate large volumes of nonwetting phase into discontinuous portions. Therefore, it is to be expected that the apparent wetting-phase saturation curve is described better by the model of Brooks and Corey than by van Genuchten's model since the latter predicts a much more gradual increase in discontinuous nonwetting phase with increasing matric potential head.

Figure 4 shows discontinuous air saturations estimated with the CNP_BCB model from the air permeability data measured for the quartz sand mixture and for both wetting and drying and involving pure water as well as an aqueous solution containing 6% butanol as the wetting fluid. Notice the substantial difference between wetting and drying. Apparently, much larger amounts of discontinuous air existed during drying, and at much lower water saturations, than during wetting. This finding agrees with the observed hysteresis in the corresponding water retention and air permeability functions (Dury, 1997, unpublished data), indicating that nonwetting-phase trapping is an important factor contributing to hysteresis. Given the values of the emergence and extinction points of air flow as derived from the air permeability experiments (Table 1), in cases like those shown in Fig. 4 it might be difficult to determine the amount of discontinuous air at nonzero air permeabilities during wetting, while it should be possible to determine this quantity during drying.

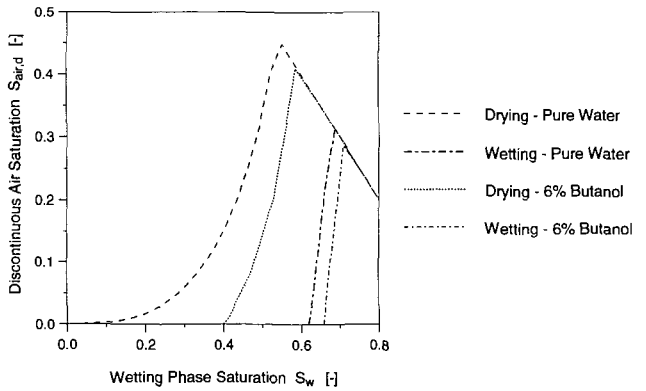

Fig. 4. Discontinuous air saturations, $S_{air,d}$, calculated from the relative air permeability data measured for the quartz sand mixture during wetting and drying involving pure water as well as an aqueous solution containing 6% butanol as the wetting fluid. The functions of $S_{air,d}$ were obtained with Eq. [6] using the Brooks and Corey–Burdine formulation of the Continuous Nonwetting Phase (CNP_BCB) model.

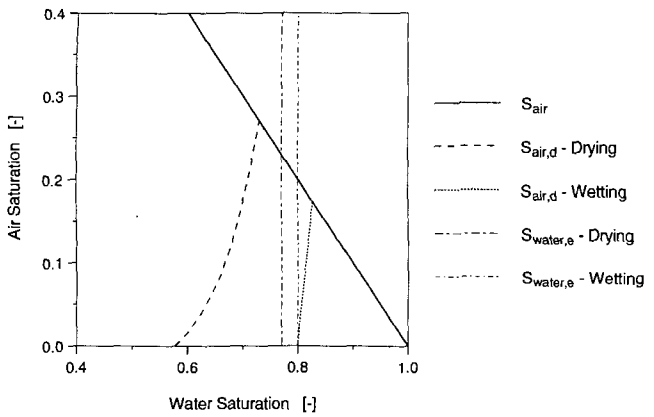

Fig. 5. Discontinuous air saturations, $S_{air,d}$, calculated from relative air permeability data determined by Stonestrom and Rubin (1989b) for Oakley sand during both wetting and drying. The functions of $S_{air,d}$ were obtained with Eq. [6] using the Brooks and Corey–Burdine formulation of the Continuous Nonwetting Phase (CNP_BCB) model. The total air saturation, S_{air}, and the experimentally determined emergence and extinction points, $S_{water,e}$, are also shown.

Figure 5 shows discontinuous air saturations calculated using the CNP_BCB model for wetting and drying air permeability data presented by Stonestrom and Rubin (1989b) for Oakley sand. Compared with the curves shown in Fig. 3 and 4, the discontinuous air saturation during drying approaches zero at much higher water saturations, while during wetting again a steep increase in the discontinuous air saturation is apparent at water saturations close to the extinction point. The calculated emergence and extinction of continuous air did not agree as much with the air permeability emergence and extinction points, respectively, as was the case in Fig. 3 for the data obtained for the quartz sand mixture, but notice that the experimental determination of emergence or extinction points strongly depends on the resolution in the nonwetting-phase permeability data. Still, the curves presented in Fig. 5 again agree with the observed hysteresis in the corresponding water retention and air permeability functions as reported by Stonestrom and Rubin (1989a,b).

Comparison of CNP_BCB, TNP, and EP Models

We tested the CNP_BCB model and compared its performance with the TNP and EP models. In Fig. 6 both models are compared with the data obtained for the quartz sand mixture during drying and involving pure water. The exponent b in both models was either fixed to 0.5 or was optimized. Notice that the EP model describes the data much better than the TNP model, irrespective of whether or not b was fixed or optimized. Even the optimized TNP model does not describe the data correctly. Optimization of b only marginally improved the fit of the EP model to the data. The main difference between the TNP and EP models is the inclusion of the discontinuous nonwetting phase in the EP model. Hence, the results of Fig. 6 illustrate the need to include the effects of a discontinuous nonwetting phase when developing nonwetting-phase relative permeability models. Similar results as those shown in Fig.

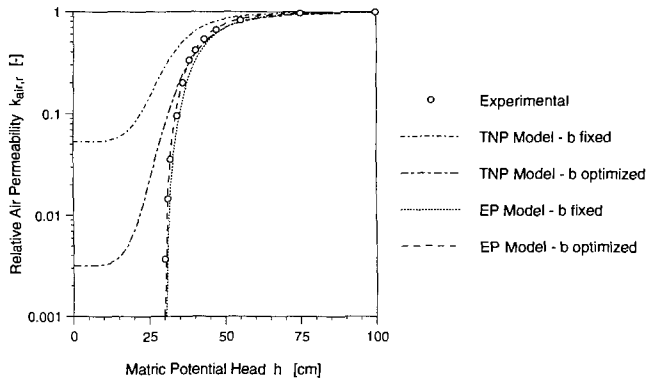

Fig. 6. Comparison of relative air permeabilities determined for the quartz sand mixture and pure water during drying with model calculations obtained with the Total Nonwetting Phase (TNP) and Emergence Point (EP) models for both a fixed and optimized exponent b. Fitted values of b are given in Table 2.

6 were obtained for all other data sets investigated in this study.

Predictions using the CNP_BCB, the TNP, and the EP models were done for the air permeability data determined for the quartz sand mixture during drying using aqueous solutions containing either 2 or 6% butanol. The matric potential head at the emergence point in the CNP_BCB model was calculated as

$$h_s(S_{w,e}) = \frac{\sigma_{2,6}}{\sigma_0} h_0(S_{w,e}) \qquad [14]$$

where $h_s(S_{w,e})$ is the scaled matric potential head at the emergence point of the aqueous solutions containing 2 or 6% butanol, $\sigma_{2,6}$ is the corresponding interfacial tension, $h_0(S_{w,e})$ is the matric potential head at the emergence point determined for pure water, and σ_0 is the interfacial tension of pure water. In the CNP_BCB model, we furthermore used the values of b and λ_a as fitted for pure water. Since the data measured for the quartz sand mixture did not indicate a significant dependence of the emergence point on wettability, for the EP model we used the same values of the emergence point as determined for pure water, took the value of b as fitted for pure water, and used the value of m obtained from fitting the retention data of the aqueous solutions containing 2 or 6% butanol. In the TNP model, we used the value of b as fitted for pure water. Those predictions were compared with calculations in which b was fixed to 0.5 in the TNP and EP models and to 2.0 in the CNP_BCB model while keeping the other parameters as described above.

Figure 7 compares drying branch data obtained for the aqueous solution containing 2% butanol with predictions obtained with the TNP, EP, and CNP_BCB models using either fixed values of b or the values as optimized for pure water. The TNP model describes the higher relative permeability data somewhat better than the CNP_BCB and the EP models when a fixed value of b was used in all three models (Fig. 7a) while this model fails to predict the low permeability data, which are described quite well by the other two models. The CNP_BCB model with fixed b slightly overestimates the permeability data in the high range while the EP

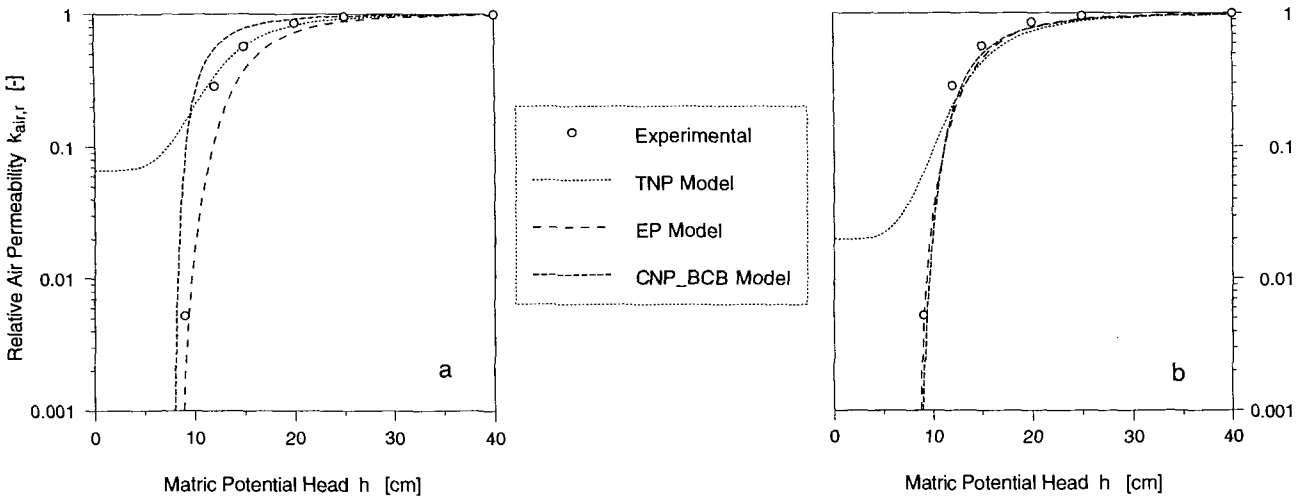

Fig. 7. Comparison of relative air permeabilities determined for the quartz sand mixture during wetting involving an aqueous solution containing 2% butanol as the wetting fluid with model predictions (see text) obtained with the Brooks and Corey–Burdine formulation of the Continuous Nonwetting Phase (CNP_BCB), Total Nonwetting Phase (TNP), and Emergence Point (EP) models. The exponent *b* was either (a) fixed to 2.0 in the CNP_BCB model and to 0.5 in the TNP and EP models or (b) the values optimized for pure water were used.

model underestimates those data. Using the values of *b* as optimized for pure water resulted in good predictions with the EP and CNP_BCB models across the entire range of permeability data (Fig. 7b). Again the optimized TNP model does not describe the data correctly. This finding shows that *b* generally is a fitting parameter but that for the same porous medium, the same process, and the same model, one single value may serve as a good estimate to describe nonwetting-phase relative permeability in the presence of wetting fluids with different wettability. Similar results as those shown in Fig. 7 were also obtained for wetting as well as the case when water containing 6% butanol was used as the wetting fluid. Generally, the predictions obtained with the EP model were as good as those calculated with the CNP_BCB model, indicating that the EP model is a good approximation of the continuous nonwetting-phase concept.

For a general predictive application of the CNP model, experimental procedures for determining continuous and discontinuous nonwetting-phase contents have to be developed. When an accurate description of relative permeability data is required for modeling purposes (e.g., Fischer et al., 1996), the CNP model can be used by fitting all three parameters as discussed above. We compared this option of the CNP_BCB model to calculations obtained with the EP model using a fitted value of *b*. In all cases, the CNP_BCB model described the data slightly better than the EP model.

CONCLUSIONS

The results presented here show that nonwetting-phase relative permeability should be modeled as a function of the continuous nonwetting-phase saturation rather than of the total nonwetting-phase saturation. Large differences between these two approaches were obtained in cases of low emergence or extinction points of the nonwetting-phase permeability. The calculated contents of discontinuous nonwetting phase suggested a more accurate description of the dependence of apparent wetting-phase saturation on matric potential head by the model of Brooks and Corey than that of van Genuchten. Our calculations indicated that during drying, considerable amounts of discontinuous nonwetting phase may exist at relatively low wetting-phase saturations, while during wetting, discontinuous nonwetting phase may exist only at wetting-phase saturations close to (as well as above) the emergence or extinction point of the nonwetting-phase permeability. This result is consistent with the observed hysteresis in the wetting-phase retention and nonwetting-phase permeability functions, indicating that nonwetting-phase trapping is a major factor determining hysteresis. The experimental determination of discontinuous nonwetting-phase content might be difficult for the wetting process while it should be more easy for drying. There is a strong need to develop such methods for a general predictive application of the CNP model.

The use of the TNP model for predictions may lead to drastic overestimation of the nonwetting-phase permeability, especially when the emergence or extinction point of the nonwetting-phase permeability is low. The EP model provided a good approximation of the CNP model and can be used when the emergence or extinction point is known. Improved methods for rapidly estimating the emergence or extinction point would be helpful. Still, even when the emergence or extinction point is known, methods for estimating the exponent *b* accounting for tortuosity and connectivity are missing. In order to improve the predictive capability of parametric permeability models, methods for estimating this parameter or new concepts accounting for tortuosity and connectivity may have to be developed.

APPENDIX

a	tortuosity exponent for the wetting phase
b	tortuosity exponent for the nonwetting phase
h	matric potential head [L]

h_a empirical parameter in the CNP_BCB model [L]
$h(S_{w,e})$ matric potential head at the emergence point [L]
$h_s(S_{w,e})$ scaled matric potential head at the emergence point [L]
$h_0(S_{w,e})$ matric potential head at the emergence point for pure water [L]
$k_{air,r}$ relative air permeability
$k_{n,r}$ relative nonwetting-phase permeability
$k_{w,r}$ relative wetting-phase permeability
m van Genuchten parameter for the wetting phase
m_a van Genuchten parameter for the apparent wetting phase
n van Genuchten parameter for the wetting phase
n_a van Genuchten parameter for the apparent wetting phase
S_{air} air saturation
$S_{air,c}$ continuous air saturation
$S_{air,d}$ discontinuous air saturation
S_n nonwetting-phase saturation
$\overline{S}_n$ effective nonwetting-phase saturation
$\overline{S}_{n,c}$ effective continuous nonwetting-phase saturation
$\overline{S}^*_{n,c}$ estimate of the effective continuous nonwetting-phase saturation
$S_{n,d}$ discontinuous nonwetting-phase saturation
S_w wetting-phase saturation
$\overline{S}_w$ effective wetting-phase saturation
$S_{w,a}$ apparent wetting-phase saturation
$\overline{S}_{w,a}$ effective apparent wetting-phase saturation
$S_{w,e}$ emergence/extinction point of nonwetting-phase flow
$S_{w,r}$ residual wetting-phase saturation
$S_{w,s}$ maximum wetting-phase saturation
$S_{water,a}$ apparent water saturation
$S_{water,e}$ emergence point for water as the wetting fluid
α van Genuchten parameter for the wetting phase [L^{-1}]
α_a van Genuchten parameter for the apparent wetting phase [L^{-1}]
λ_a Brooks and Corey parameter for the apparent wetting phase [L^{-1}]
σ_0 interfacial tension of pure water [$M\ L^{-2}$]
$\sigma_{2,6}$ interfacial tension of aqueous solutins containing 2 or 6% butanol [$M\ L^{-2}$]

REFERENCES

Brooks, R.H., and A.T. Corey. 1964. Hydraulic properties of porous media. Hydrol. Pap. no. 3. Civil Engineering Dep., Colorado State Univ., Fort Collins.

Burdine, N.T. 1953. Relative permeability calculations from pore-size distribution data. Trans. Am. Inst. Min. Metall. Pet. Eng. 198:71–78.

Corey, A.T. 1957. Measurement of water and air permeability in unsaturated soil. Soil Sci. Soc. Am. Proc. 21:7–10.

Demond, A.H., and P.V. Roberts. 1987. An examination of relative permeability relations for two-phase flow in porous media. Am. Water Resour. Assoc. Bull. 23:617–628.

Demond, A.H., and P.V. Roberts. 1993. Estimation of two-phase relative permeability relationships for organic liquid contaminants. Water Resour. Res. 29:1081–1090.

Fischer, U., R. Schulin, M. Keller, and F. Stauffer. 1996. Experimental and numerical investigation of soil vapor extraction. Water Resour. Res. 32:3413–3427.

Lenhard, R.J., and J.C. Parker. 1987. A model for hysteretic constitutive relations governing multiphase flow. 2. Permeability–saturation relations. Water Resour. Res. 23:2197–2206.

Morgan, J.T., and D.T. Gordon. 1970. Influence of pore geometry on water–oil relative permeability. J. Pet. Technol. 22:1199–1208.

Mualem, Y. 1976. A new model for predicting the hydraulic conductivity of unsaturated porous media. Water Resour. Res. 12:513–522.

Odeh, A.S. 1959. Effect of viscosity ratio on relative permeability. Pet. Trans. 216:346–353.

Parker, J.C., R.J. Lenhard, and T. Kuppusamy. 1987. A parametric model for constitutive properties governing multiphase flow in porous media. Water Resour. Res. 23:618–624.

Stonestrom, D.A. 1987. Co-determination and comparisons of hysteresis-affected, parametric functions of unsaturated flow: Water-content dependence of matric pressure, air trapping, and fluid permeabilities in a non-swelling soil. Ph.D. diss. Stanford Univ., Stanford, CA (Diss. Abstr. 88-01040).

Stonestrom, D.A., and J. Rubin. 1989a. Water content dependence of trapped-air in two soils. Water Resour. Res. 25:1947–1958.

Stonestrom, D.A., and J. Rubin. 1989b. Air permeability and trapped-air content in two soils. Water Resour. Res. 25:1959–1969.

van Genuchten, M.Th. 1980. A closed-form equation for predicting the hydraulic conductivity of unsaturated soils. Soil Sci. Soc. Am. J. 44:892–898.